

# Vibrational Fine Structure in C 1s High-Resolution Core-Level Spectra of CO Chemisorbed on Ir(111)

Stefania Baronio, Valeria De Leo, Ginevra Lautizi, Paola Mantegazza, Eleonora Natale, Manuel Tuniz, Stefano Vigneri, Luca Bignardi, Paolo Lacovig, Silvano Lizzit, and Alessandro Baraldi\*



Cite This: *J. Phys. Chem. C* 2022, 126, 1411–1419



Read Online

ACCESS |



Metrics & More

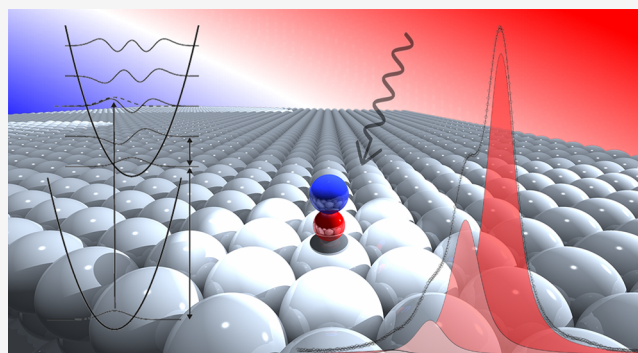


Article Recommendations



Supporting Information

**ABSTRACT:** The vibrational features of carbon monoxide (CO) adsorbed on Ir(111) were studied by means of high-resolution core-level spectroscopy. By monitoring the Ir  $4f_{7/2}$  core level as a function of exposure, we proved that the CO adsorbs on the surface always in on-top sites, in agreement with the results of vibrational spectroscopy techniques and density functional theory studies. The C 1s vibrational splittings measured for the  $p(\sqrt{3} \times \sqrt{3})R30^\circ$  ( $233.4 \pm 0.5$  meV) and  $c(4 \times 2\sqrt{3})\text{rect}$  ( $231.4 \pm 0.4$  meV) structures were in good agreement with the  $Z + 1$  model. Despite the very small error bar of the measurements, it was not possible to reveal any anharmonic contribution to the spectral lineshape. We speculate that the contribution of the unresolved vibrational mode of the frustrated translation or the effect of phonon-mediated interaction with the substrate can account for the observation of this outcome.



the observation of this outcome.

## INTRODUCTION

The investigation of vibrational properties of molecules and solids typically relies on infrared-radiation spectroscopies or monochromatized electron energy loss spectroscopy experiments. However, since the pioneering experiments of Siegbahn and co-workers in the 1970s,<sup>1–3</sup> it has been understood that the vibrational fine structure in simple molecules in the gas phase also can be detected by means of high-resolution X-ray photoelectron spectroscopy (HR-XPS). The photoionization process is accompanied by vibrational excitation caused by the presence of a localized hole that induces a strong rearrangement of the electron density distribution in the excited molecule. It has been observed for the specific case of carbon monoxide (CO) that the vibrational fine structure is strongly dependent on the photon energy of the X-radiation used for the experiment. This happens particularly in the supra-threshold region, where resonance effects may dominate over those caused by the differential cross section. In the gas phase this phenomenon is particularly enhanced for energies of  $\sim 310$ – $315$  eV and leads to measurements of an energy of  $301 \pm 3$  meV between the ground state  $\nu' = 0$  and the first excited state  $\nu' = 1$  of the carbon core-ionized CO molecule.<sup>4</sup> This value is in excellent agreement with the value predicted by the  $Z + 1$  equivalent core model of 307.5 meV.<sup>5</sup>

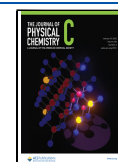
It is important to remark that, in the photoemission process, unlike the case of vibrational spectroscopy techniques, the measured vibrational excitation is the one corresponding to the excited final state, while at the typical temperature of the

experiments almost all molecules occupy only the ground state. These studies have been extended since the end of the 20th century to molecules with hydrocarbon functional groups chemisorbed on a variety of solid surfaces.<sup>6–13</sup> Such knowledge was instrumental in achieving crucial information on the properties of the adsorbate–substrate bond for a possible use in heterogeneous catalysis. Besides hydrocarbons, in which the C–H bond leads to final-state vibrational frequencies on the order of 350–400 meV, other chemisorbed molecules, such as CO, have been investigated using HR-XPS. The outcomes of these experiments showed smaller core-level vibrational splitting. The first investigation of this kind aimed to investigate the different adsorption sites of CO molecules on the Ni(100) surface. Besides the well-known chemical shift in the C 1s core level due to different adsorption sites, Föhlich et al.<sup>14</sup> revealed that the final-state vibrational frequencies were dependent on the specific adsorption configuration. In particular, on Ni(100) vibrational splittings  $E_{\text{vib}}$  equal to 217.8, 183, and 156.6 meV were found for on-top, bridge, and four-fold adsorption configurations, respectively. Successive investigations showed that vibrational splitting for molecules

**Received:** November 8, 2021

**Revised:** January 6, 2022

**Published:** January 18, 2022



adsorbed at on-top sites depends on the substrate on which the molecule is adsorbed, with values ranging from 200 up to 260 meV (see Table 1).

**Table 1. C 1s Vibrational Energies and Core Electron Binding Energies As Probed by High-Resolution X-ray Spectroscopy for CO Molecules Adsorbed in On-Top Sites on Different Transition Metal Surfaces<sup>a</sup>**

vibrational splitting (meV)	adiabatic peak (eV)	substrate	reference
301.2 ± 0.4	285.8 ± 0.1	gas phase	
217.8 ± 2.2	285.8 ± 0.1	Ni(100)	14
213	285.7	Ru(0001)	15
232 ± 2	286.04	Rh(111)	16
221 ± 4	285.68	Co(0001)	17
200	285.55	Pd(111)	18
260	286.7	Pt(111)	19
233.4 ± 0.5	286.23 ± 0.05	Ir(111)	this work
231.4 ± 0.4	286.22 ± 0.05	Ir(111)	this work

<sup>a</sup>References are reported in the last column. The two values referred to in this work correspond to the two different coverages obtained for CO on Ir(111).

In this work we investigated the adsorption of CO on the surface of Ir(111) through fast HR-XPS.<sup>20</sup> The measurements of the core-level shifts of the substrate atoms provided information on the adsorption site of the CO molecules on Ir(111). On the other hand, the C 1s high-resolution core-level spectra of CO gave insight into the molecular vibrational structure of the adsorbed molecules and the presence of anharmonic contributions. It was expected that the anharmonic correction  $\omega_e x_e$  could contribute to the vibrational frequency for a value of energy that was ~1% with respect to the vibrational splitting,<sup>21</sup> which was equivalent to measurement variations in C 1s core electron binding energies ( $\Delta E_b$ ) and required one to detect variations in binding energy on the order of 3 meV.<sup>22</sup> The achievement of such accuracy constituted a considerable experimental challenge because it demanded the measurement of C 1s core-level spectra with an excellent signal-to-noise ratio, while retaining an overall energy resolution considerably better than the vibrational splitting. Moreover, to decrease the contribution of spectral broadening caused by inhomogeneities (molecules in slightly different chemical environment), it was necessary to prepare long-range ordered surface layers with a low density of defects and with excellent degree of cleanliness, where preferably only a single adsorption site was occupied.

All of these conditions were satisfied for the adsorption of CO on the Ir(111) surface, for which it was possible to prepare large atomic terraces up to several hundreds of angstroms and to form CO long-range ordered structures at different coverages.<sup>23</sup> In the first part of our study, we prepared two structures with different periodicities and symmetries corresponding to the 0.33 ML ( $p(\sqrt{3} \times \sqrt{3})R30^\circ$  structure) and 0.42 ML ( $c(4 \times 2\sqrt{3})\text{rect}$  structure) coverage of CO. In a second step, by measuring the coverage dependence of Ir 4f<sub>7/2</sub> core-level spectra, we verified in a direct way that the site of CO adsorption is the on-top one for both ordered structures. Last, we measured the vibrational fine structure associated with the C 1s core level for both of the ordered structures that we prepared, extracting the values of the adiabatic transitions observed.

## EXPERIMENTAL METHODS

Preliminary determination of the coverage-dependent adsorption configuration was carried out by means of low-energy electron diffraction (LEED) experiments in the ultrahigh-vacuum (UHV) chamber of the Nanoscale Materials Laboratory of Elettra-Sincrotrone Trieste, a system that is equipped with both rear-view LEED and Omicron spot-profile analysis (SPA)-LEED. High-resolution core-level measurements were performed at the SuperESCA beamline of the Elettra synchrotron radiation facility in Trieste, Italy. The photoemission spectra were collected by means of a Phoibos 150 mm mean radius hemispherical electron energy analyzer from SPECS, equipped with an in-house developed delay line detector. The overall experimental energy resolution (which accounts for both the electron energy analyzer and the X-ray monochromator) was always kept below 50 meV in all measurements, as determined by probing the width of the Fermi level of an Ag polycrystal.

An Ir(111) single crystal was mounted on a sample manipulator with four degrees of freedom. The sample was heated by electron bombardment from three hot tungsten filaments mounted close to the sample back. The temperature of the sample was monitored by means of two K-type thermocouples directly spot-welded on the edges of the specimen. The Ir surface was cleaned by repeated cycles of Ar ion sputtering and flash annealing to 1400 K, followed by annealing in O<sub>2</sub> and in H<sub>2</sub> gas.<sup>24,25</sup> The surface long-range order and cleanliness were checked by LEED, which resulted in a sharp (1 × 1) pattern with low background intensity, and by X-ray photoelectron spectroscopy (XPS), which showed that adventitious Si, S, B, C, and any other contaminant were under the detection limit. From the SPA-LEED analysis, we estimated an average terrace width of ~300 Å.

Ir 4f<sub>7/2</sub> core-level spectra were acquired at  $T = 300$  K using a photon energy of 200 eV to ensure simultaneously high photoelectron yields and high surface sensitivities. C 1s spectra of adsorbed CO molecules were measured at  $T = 80$  K and with a photon energy of 307.5 eV to maximize the signal from vibrationally split components, in close agreement to what has been found in the case of the experiments performed on Ru(0001).<sup>15</sup> The photon energy  $h\nu = 307.5$  eV was chosen in the interval  $h\nu = 304\text{--}317.5$  eV in order to minimize the contribution of the background and maximize the possibility to distinguish the vibrational component from the adiabatic peak (see Figure S1 in the Supporting Information). As one can see in Figure S1, the spectrum at  $h\nu = 307.5$  eV represented the best compromise to achieve such a goal. For each spectrum, the photoemission intensity was normalized to the incoming photon flux and the binding-energy (BE) scale was aligned to the Fermi level of the Ir substrate. Doniach–Šunjić line profiles were used to fit each spectral component (which included a Lorentzian width  $\Gamma$  and the Anderson asymmetry parameter  $\alpha$ ), convoluted with a Gaussian distribution, which accounted for the experimental, phonon, and inhomogeneous broadening.<sup>26</sup> For the Ir 4f<sub>7/2</sub> core-level spectra measured at 200 eV photon energy, the background was subtracted using a linear fit, a widely accepted procedure for Ir(111).

## RESULTS AND DISCUSSION

**Long-Range Ordered CO-Induced Structures.** The ordered structures formed by CO on Ir(111) investigated in this work corresponded to two different coverages. The low

coverage phase, corresponding to the  $p(\sqrt{3} \times \sqrt{3})R30^\circ$  periodicity,<sup>23,27–31</sup> was obtained by using a strategy that allowed for easy diffusion of CO molecules on the metal surface, which consequently led to the formation of an overlayer structure with better ordering. The CO exposure started at a pressure of  $4 \times 10^{-8}$  mbar with the substrate at 620 K. Subsequently, the crystal was cooled (with a rate of 4 K/s) down to 120 K, at which the CO exposure was stopped. Last, the sample was flashed up to 590 K. The optimal temperature for the final annealing procedure was chosen in the range 350–670 K on the basis of the analysis of the intensity and full width at half-maximum of the CO-induced electron diffraction spots, measured at room temperature.

The high-coverage CO-induced ordered structure can be described as a  $c(4 \times 2\sqrt{3})\text{rect}$  or, according to the Park formalism, as a  $\begin{pmatrix} 3 & 1 \\ 1 & 3 \end{pmatrix}$  structure. This phase was prepared using the same procedure of the low-coverage structure but with a different temperature for the final annealing (230 K). The LEED pattern of the two structures, acquired at 80 K, is reported in Figure S2. The CO-coverage calibration was obtained assuming that the  $p(\sqrt{3} \times \sqrt{3})R30^\circ$  structure corresponded to a coverage of 0.33 ML. On the basis of the C 1s photoemission measurements, we assigned to the  $c(4 \times 2\sqrt{3})\text{rect}$  structure a coverage of 0.42 ML. Depending on the number of CO molecules that one can add in the  $c(4 \times 2\sqrt{3})\text{rect}$  unit cell above the minimum coverage of 0.125 ML, i.e., 2 molecules for each 16 Ir atoms, one can form a  $c(4 \times 2\sqrt{3})\text{rect}$  structure with the same symmetry and periodicity but with a higher coverage. The inclusion of 7 atoms yielded a stoichiometric ratio of 7 CO/16 Ir, i.e., with a coverage of 0.437 ML, which was very close to the value we found experimentally.

**Determination of the CO Adsorption Site.** Prior to investigating the vibrational properties of the CO molecules in the two ordered structures, we provided further evidence that CO adsorbed on Ir(111) in the on-top configuration, independently from the coverage. Techniques such as high-resolution electron energy loss spectroscopy (HR-EELS) and infrared (IR) spectroscopy concluded that the CO molecules preferred a single-site adsorption configuration, the on-top one, a result that also was supported by theoretical calculations performed within the density functional theory framework.<sup>32–35</sup> This outcome differed from that of Pt(111), for which it was known that, although the on-top configuration was preferred at low coverage, the CO molecules tended to populate also the bridge sites at high coverages.<sup>36–38</sup>

The determination of the CO adsorption site was conducted following a method already used to individuate the adsorption site of atoms and molecules on transition metal surfaces. This consisted of the analysis of the evolution of the coverage-dependent intensities of the  $3d_{5/2}$  and  $4f_{7/2}$  surface core-level shifted components for the 4d and 5d transition metal surfaces, respectively.<sup>24,39,40</sup>

In the initial part of the investigation, a set of Ir  $4f_{7/2}$  core-level spectra was acquired at normal emission ( $h\nu = 200$  eV) after adsorption at  $T = 300$  K of different amounts of CO up to saturation, as shown in Figure 1. The spectrum of the clean Ir(111) was characterized by two components that we assigned to bulk ( $\text{Ir}_B$  component with binding energy (BE) =  $60.802 \pm 0.015$  eV) and first-layer Ir atoms ( $\text{Ir}_S$  component with BE =  $60.259 \pm 0.015$  eV) with a surface core-level shift (SCLS) (that is, the BE difference between surface and bulk atoms)

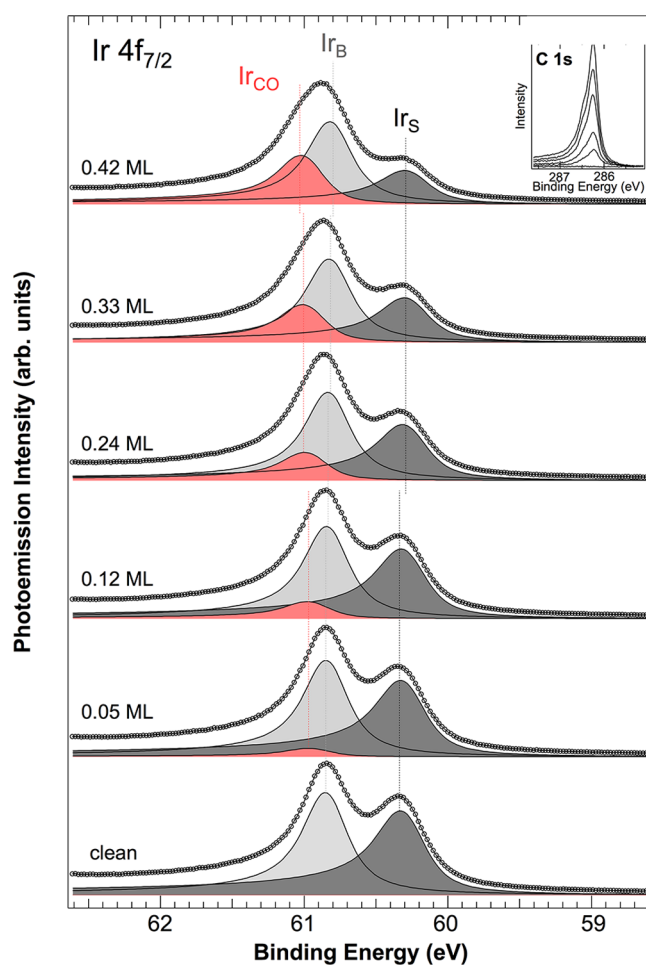


**Figure 1.** Ir  $4f_{7/2}$  core-level spectra from the Ir(111) surface acquired at 200 eV photon energy and  $T = 300$  K, after exposures of carbon monoxide and a subsequent increase of the annealing temperature to induce the partial CO desorption and produce coverages ranging from 0 to 0.42 ML. Three different components can be individuated, originating from bulk atoms (light gray), clean surface atoms (dark gray), and first-layer Ir atoms bonded to CO (red). The corresponding sequence of C 1s core-level spectra of CO molecules, used for coverage calibration, is reported in the top-right inset.

equal to  $-543 \pm 15$  meV, in agreement with earlier experiments.<sup>24,25</sup> As for the adsorption of atoms and molecules on many transition metal surfaces,<sup>41</sup> the CO adsorption on Ir(111) was characterized by a clear decrease in the component  $\text{Ir}_S$  and the appearance of a new component  $\text{Ir}_{CO}$  at a different BE. In our specific case we detected a new surface core-level shifted component growing at  $+180 \pm 15$  meV, with respect to  $\text{Ir}_B$ , which we attributed to the formation of the Ir–CO bond. It is important to underline that, in the entire coverage range from the clean surface until saturation, this was the only additional component growing in the Ir  $4f_{7/2}$  spectrum. This trend was analogous to the evolution of the Pt  $4f_{7/2}$  core-level spectra upon CO adsorption on Pt(111) at low coverage.<sup>42</sup> For that system, the SCLS corresponding to the clean surface was  $-0.4$  eV. Upon low coverage deposition and formation of a  $(4 \times 4)$  CO long-range ordered structure with a coverage of 0.2 ML, where the CO molecules occupied an on-top site, an additional component appeared at 71.91 eV, i.e., at  $\sim 1$  eV higher BE than for the bulk component, while the growth of a second peak at 71.23 eV was explained with the

occupation of a bridge site. This was a preliminary indication that, unlike in the case of Pt(111), there was only one configuration of CO adsorption on the surface of Ir(111). It is interesting to report that the residuals of the fit improved by imposing a linear overlay dependence on the position of the bulk component (25 meV from clean to saturation), which prompted the hypothesis that the second-layer atoms may have been affected slightly by the adsorption of CO. It is realistic to assume that Ir atoms adjacent to and underlying other Ir CO-bound atoms could sense an electronic charge redistribution and, hence, a first-to-second layer distance modification could take place. On the other hand, the SCLS remained unaltered (545 meV) within the error bar of 20 meV. The best line-shape parameters for the bulk ( $\text{Ir}_B$ ) and surface components ( $\text{Ir}_S$  and  $\text{Ir}_{CO}$ ) are reported in Table 2.

**Table 2. Ir  $4f_{7/2}$  Lineshape Parameters (Lorentzian Width  $\Gamma$ , Anderson  $\alpha$  Asymmetry, Gaussian Width  $G$  for the Bulk, Surface, and CO-Induced Surface Peaks**

	$\text{Ir}_B$	$\text{Ir}_S$	$\text{Ir}_{CO}$
$\Gamma$ (meV)	297	249	179
$\alpha$	0.091	0.209	0.209
$G$ (meV)	144	202	224

The larger value of the Anderson  $\alpha$  parameter for the surface components can be explained by the higher density of states projected on the surface atoms, which may result in a larger probability to create electron–hole pairs. However, it is to be noted that the numeric value of  $\alpha$  might be affected by the choice of type of background (e.g., Shirley) used for the fit. For all components the Gaussian contributions are clearly much larger than the experimental resolution. It is worth noting that the Gaussian contribution to the spectral line width is caused by experimental broadening but also by phonon (thermal) broadening and by broadening due to the inhomogeneity in the systems (presence of nonequivalent configurations). These effects are also expected to produce a larger Gaussian contribution for the  $\text{Ir}_S$  components than for the  $\text{Ir}_B$  because

of the phonon broadening, as already observed for surfaces of alkali<sup>45</sup> and other transition metals.<sup>44,45</sup> The reduced Lorentzian width  $\Gamma$  of the new  $\text{Ir}_{CO}$  component could be ascribed to the role played by the bond formed between Ir atoms and CO in modifying the core–hole lifetime.

To determine in a direct way the CO adsorption site, a sequence of Ir  $4f_{7/2}$  core-level spectra ( $\sim 90$  spectra, shown in Figure 2a) were acquired while exposing the surface kept at  $T = 300$  K to increasing CO pressure, as reported in Figure 2b. The pressure used for the uptake was quite low at the beginning of the process in order to detect even minimal modifications in the core-level lineshape, considering that the adsorption process is quite fast. The pressure was then increased up to  $4 \times 10^{-8}$  mbar, when the surface saturation for room temperature was almost achieved.

The accurate preliminary determination of the core-level lineshape achieved in the first part of our experiment (Figure 1) was pivotal to fit the whole series of spectra constraining the lineshape parameter of the three Ir components while letting only the intensity of the 3 peaks change as a free parameter of the fit (together with a variable background, slope, and intercept). The BE of the bulk component was varied in a linear way according to the behavior for the high-resolution spectra. The evolution of the bulk  $\text{Ir}_B$  and surface components ( $\text{Ir}_S$  and  $\text{Ir}_{CO}$ ), as a result of the fitting procedure, is reported in Figure 2c–e. The decrease in the intensity of the  $\text{Ir}_B$  (Figure 2c) is easily attributable to the screening effect exerted by the CO molecules adsorbed on the surface, which reduced the probability of the photoelectrons emitted from the second and deeper atomic layers reaching the detector. On the other hand, the reduction of the  $\text{Ir}_S$  component (Figure 2d) was caused by the reduction of the population of Ir atoms belonging to the first layer that were clean, i.e., did not form any bonds with CO molecules. At the same time, and as expected, the number of atoms from the first surface layer bound to a CO molecule increased as the amount of adsorbed CO increased (Figure 2e).

A series of C 1s core-level spectra during CO exposure was collected contextually to the Ir 4f spectra (see Figure S3), so

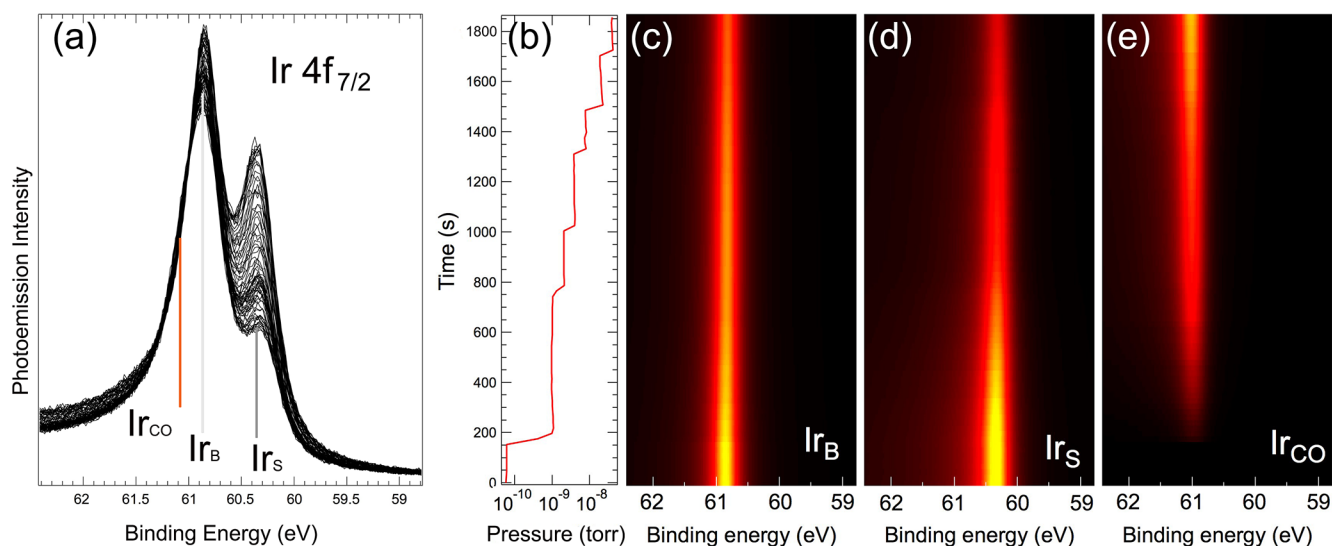


**Figure 2.** (a) Sequence of Ir  $4f_{7/2}$  core-level spectra from Ir(111) surface recorded at 200 eV photon energy and  $T = 300$  K during the adsorption of CO. (b) Evolution of the CO pressure during the uptake. (c) 2D plot of the results of the spectral analysis of the core-level spectra for the (c)  $\text{Ir}_B$  component, (d)  $\text{Ir}_S$  surface component, and (e)  $\text{Ir}_{CO}$  component.

that we could report the intensity trend of the  $I_{r_s}$  versus exposure (normalized to 1 for the spectrum acquired on the clean surface) as the CO coverage increased. Once we obtained the two trends of  $I_{r_s}$  and C 1s versus exposure, we used an interpolation process on the exposure data and obtained the plot of the evolution of  $I_{r_s}$  vs CO coverage.

The evolution of  $I_{r_s}$  versus the CO coverage is shown in Figure 3. From the graph it is evident that the intensity of this

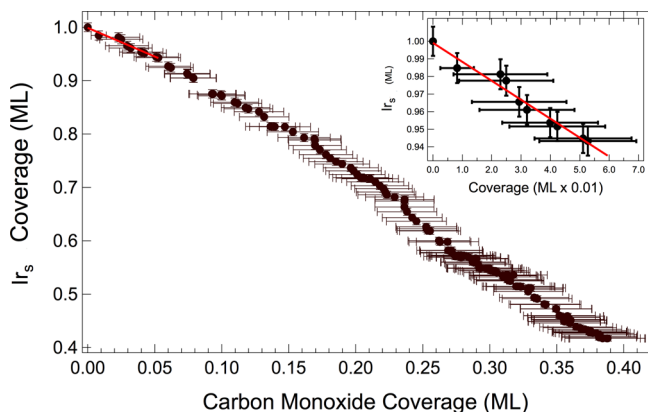


**Figure 3.** CO-coverage-dependent intensity of the  $I_{r_s}$  component, normalized to 1, as obtained by fitting the spectral sequence shown in Figure 2a. The first derivative  $\frac{\partial I_{r_s}}{\partial \Theta_{CO}}$ , calculated for low coverage, is equal to  $-1.08$ .

component decreased linearly with increasing CO coverage, in particular at the early stages of the adsorption process. A linear fit of the curve was carried out in the initial part, more specifically up to 0.05 ML coverage. The resulting value of the slope of the curve in this range was  $\frac{\partial I_{r_s}}{\partial \Theta_{CO}} = -1.08 \pm 0.16$ , i.e., a value fully compatible with the value of  $-1$ , which was expected in the case of CO adsorption in on-top sites: for each CO molecule adsorbed on Ir(111), one Ir atom of the clean surface  $I_{r_s}$  was converted into  $I_{r_{CO}}$ . The data analysis on the slope of the curve describing the trend of  $I_{r_s}$  was carried out specifically at the beginning of the CO uptake. The motivation behind it was the influence of photoelectron diffraction effects taking place when the CO coverage increased. Consequently, the intensity of the Ir surface atoms without an adsorbed CO molecule ( $I_{r_s}$ ) was affected by the presence of CO molecules adsorbed on surface Ir first neighbors. Thus, if the CO coverage was very large, the measured photoemission intensity sourcing from  $I_{r_s}$  did not decay in a linear fashion.<sup>39,46</sup>

**C 1s Vibrational Levels.** To study the vibrational effects and assess the presence of anharmonicity, we measured the C 1s spectra of the two structures at low and high CO coverages at an energy of 307.5 eV while keeping the sample at  $T = 80$  K. The low-temperature measurements were essential to reduce the phonon-induced broadening in the core levels. The spectra obtained from this experiment are shown in Figure 4 (after background subtraction) along with the results of the data analysis including the different vibrational components and the residuals.

The background was described with different polynomial functions in order to take into account the presence of a large amount of secondary electrons because the C 1s spectra were acquired here with an electron kinetic energy of  $\sim 20$  eV. To do this, we applied a mask to each spectrum in order to perform a

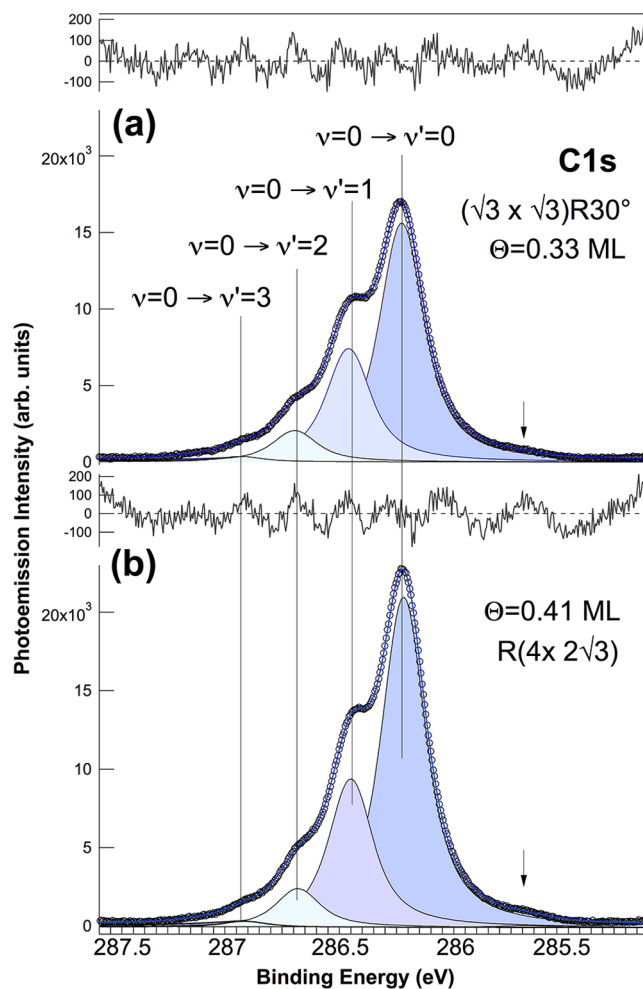


**Figure 4.** High-resolution C 1s core-level spectra for the (a)  $p(\sqrt{3} \times \sqrt{3})R30^\circ$  at 0.33 ML and (b)  $c(4 \times 2\sqrt{3})\text{rect}$  at 0.41 ML ordered structures. The adiabatic peak is shown together with the replicas for the various vibrational quantum excitations. The photon energy used was  $h\nu = 307.5$  eV. The black curves above each photoemission spectrum are the fit residuals. The arrow at  $\sim 285.7$  eV indicates the presence of a low-intensity component, which can be due to the occupation of CO molecules of bridge, three-fold sites or defective sites.

fit only in the regions where the background was dominant and the C 1s spectral weight was strongly reduced, that is, at higher ( $>287.3$  eV) and lower ( $<285.5$  eV) binding energies. The best results, compatible with the strategy to minimize the number of degrees of freedom, were obtained by using a third-degree polynomial.

After background subtraction, we made a first fit considering the presence of 4 components with the same lineshape. This choice was justified by the fact that they appeared as the most intense: the main component was the adiabatic peak ( $\nu = 0 \rightarrow \nu' = 0$  transition) at 286.227 eV, sided by three vibrational replicas at higher BE due to the transitions from the  $\nu = 0$  initial state to the  $\nu' = 1, 2$ , and 3 excited states. However, to reduce the modulation in the residual, especially in the low BE range, we decided to add an additional component (always with the same lineshape) that was visible in both spectra at 285.7 eV (indicated by a black arrow). We speculated that the presence of this component was caused by CO molecules adsorbed in other adsorption sites, in particular, in surface

defects, especially when the CO–metal bond was localized on the monatomic steps or in the case of occupation of three-fold or bridge sites, for which it is known that CO shows a value of the C 1s BE that is always lower than that of the on-top site. The initial-stage data analysis allowed us to understand that the Anderson asymmetry parameter  $\alpha$  tended to be always close to zero. To avoid any meaningless result (extremely small value of  $\alpha$  parameter, but negative), we decided to keep the value of  $\alpha$  at zero. This value is not far from the one used by Smedh et al. (0.04) for the case of CO adsorbed on Rh(111).<sup>16</sup>

The best estimate for the lineshape parameter, the position of the vibrational components, and the relative error bars can be obtained by analyzing the correlation that is commonly found between the Lorentzian and Gaussian contributions to the core-level spectral width. This effective method has been successfully applied for other systems<sup>24,47</sup> and consists of evaluating the trend of the  $\chi^2$  obtained from the single fits when the two fitting parameters are simultaneously varied. We constructed a two-dimensional grid centered on the best values ( $\Gamma_{\text{best}} = 185$  meV,  $G_{\text{best}} = 100$  meV) obtained from the previous fits. For each point of the  $n \times m$  grid, corresponding to a different pair of values of the Lorentzian and Gaussian widths, a fit to the experimental data was performed. The fits were performed while constraining the parameters  $\Gamma_n$  and  $G_m$  to the value of each point in the grid and  $\alpha = 0$ , while the other parameters were left free. The purpose of this procedure was to produce a  $\chi^2$  contour plot and to build a two-dimensional map of a third parameter—in our specific case, the binding energy of the adiabatic component and the quantum excitation energies—in order to analyze their evolution as a function of the parameters  $\Gamma$  and  $G$ . For clarity, the maps plotted in color scale reported in Figure 5 show the trend of the BE of the

calculation of the corresponding range of variations in the fitting coefficients. Moreover, it is possible to appreciate from the observation of the contour lines the correlation between the Gaussian and Lorentzian parameters, which can be inferred from the presence of a clear minimum of  $\chi^2/\chi_{\text{min}}^2$  with an elliptical shape. The values of the best fitting parameters with the error bars are reported in Table 3.

**Table 3. Fitting Parameters for the Two Ordered Structures Obtained from the  $\chi^2$  Analysis**

	$p(\sqrt{3} \times \sqrt{3})R30^\circ$	$c(4 \times 2\sqrt{3})\text{rect}$
$E_{\text{adiab}}$ (eV)	286.227	286.219
$\nu' = 0 \rightarrow \nu' = 1$ (meV)	$233.4 \pm 0.5$	$231.4 \pm 0.4$
$\nu' = 0 \rightarrow \nu' = 2$ (meV)	$467.9 \pm 1.2$	$462.5 \pm 1.1$
$\nu' = 0 \rightarrow \nu' = 3$ (meV)	$707.2 \pm 2.7$	$696.1 \pm 2.4$

These quantitative results highlighted that for both coverages the energy of the excitation when measured in photoemission was very different from the energy of the vibrational frequencies measured in electron energy loss experiments, which were found to be in the range between 250 and 270 meV. A more appropriate comparison should be made instead with the vibrational frequencies in the NO molecule adsorbed in on-top sites on the surface of Ir(111), for which a value of 230 meV was reported,<sup>48,49</sup> in excellent agreement with our results. The result can be interpreted in the framework of the  $Z + 1$  model, for which the removal of an electron from a deep core level was interpreted as an additional charge around the nucleus interacting with the remaining  $N - 1$  electrons. It is also worth mentioning the value of the natural Lorentzian width (185 meV), which was almost twice the value commonly accepted for CO in the gas phase, ranging from 90 to 97 meV.<sup>50,51</sup> This suggested that the lifetime of the core hole was strongly influenced by the electronic high density of states available at the Fermi energy on the Ir surface.

The measurement of vibrational frequencies led to the determination, in the regime of harmonic approximation, of the  $S$  factor, which is defined as  $S = \frac{\mu\omega m}{2h}(\Delta r)^2$ , where  $\mu$  is the reduced mass,  $\Delta r$  is the change of the minimum in the potential energy curve upon excitation,  $m$  is the number of C–O bonds (in this case  $m = 1$ ), and  $\omega$  is the vibrational frequency in the ground state.<sup>52</sup> The outcomes of this analysis evidenced that  $S$ , the intensity ratio of the first vibrationally excited state and the adiabatic peak, changed ca. 10%, going from 0.474 for 0.33 ML down to 0.449 for 0.42 ML. This implied that the change in the bond length  $\Delta r$  caused by the excitation was larger when the coverage was small (0.048 Å), while for larger coverage we obtained a value of  $\Delta r = 0.046$  Å.

Despite the fact that the energies of the vibrational quanta were measured with a small error bar, it was not possible to infer any contribution due to anharmonic terms in the interaction potentials. The results obtained were indeed fully consistent with the assumption that only harmonic effects took place. The absence of any anharmonic contributions in the interaction potential could be attributed to the difference between adsorbed molecules and molecules in the gas phase. A very important effect happening for the molecules adsorbed on the surface layers was certainly related to the vibrational mode of frustrated translation, associated with the movement of the whole molecule parallel or perpendicular to the surface plane, and to a lower extent to rotational motions. The energies of the

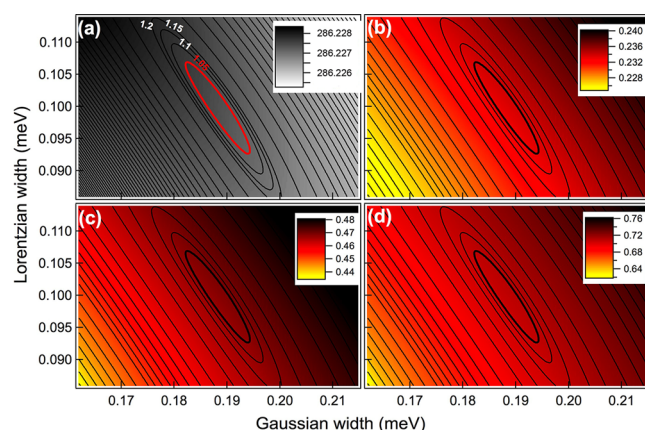


**Figure 5.**  $p(\sqrt{3} \times \sqrt{3})R30^\circ$  CO structure. Two-dimensional maps refer to (a) the binding-energy position of the adiabatic peak and the (b) first, (c) second, and (d) third excitation energies in the final states as a function of the Lorentzian  $\Gamma$  and Gaussian  $G$  width of each component. The plots are overlapped with the contour plot of the normalized  $\chi^2/\chi_{\text{min}}^2$ .

adiabatic peak (a) and of first- (b), second- (c), and third- (d) vibrational excitations, on which the contour plots of  $\chi^2/\chi_{\text{min}}^2$  (black curves) are superimposed. We specifically show the case of the  $p(\sqrt{3} \times \sqrt{3})R30^\circ$  structure, but the same line of reasoning applies identically to the  $c(4 \times 2\sqrt{3})\text{rect}$  structure.

This method is also very useful for evaluating the error bar that affects the fitting parameters: the region where the  $\chi^2$  lays within 5% from its minimum value ( $\chi^2/\chi_{\text{min}}^2 < 1.05$ ) allows the

first modes typically were in the thermal energy regime (<20 meV) and, as such, were expected to be occupied even at temperatures below 100 K. Such a low-energy excitation could influence the overall spectral lineshape and hide the effect of the anharmonic terms. In addition to that, one has to consider the possibility of shake-up or shake-off processes, which were very evident in the case of low coupling systems (i.e., in the gas phase), but that cannot be totally neglected even in the case of molecular chemisorption. Moreover, the phonon-mediated adsorbate–adsorbate interactions could also play a role. A further possibility can be found in the presence of surface defects, which can induce an inhomogeneous distribution, albeit small, of C 1s spectral components. We refer in particular to the occupation of on-top sites where the configuration of the nearest-neighbors was not exactly the same, resulting in low-intensity spectral components at slightly different binding energies, which were not included in the fit. In this respect, Li et al.<sup>29</sup> highlighted how CO molecules on Ir(111), because of dipole–dipole lateral interactions, can change their inclination with respect to the normal to the surface. This phenomenon, which for the coverage investigated in our experiments was evaluated to lead to inclinations of  $\sim 20^\circ$ , could thus also affect the binding energy of the adsorbate C 1s core levels.

## CONCLUSION

We have studied the adsorption of CO on Ir(111) by means of high-resolution X-ray photoelectron spectroscopy. First of all, we characterized the two different structures, namely,  $p(\sqrt{3} \times \sqrt{3})R30^\circ$  and  $c(4 \times 2\sqrt{3})\text{rect}$ , formed by CO on Ir(111) depending on the coverage (0.33 and 0.42 ML, respectively). We confirmed that CO adsorbs on the Ir(111) surface in on-top sites for both of the observed structures. Information about the vibrational properties of CO were obtained by acquiring high-resolution spectra of the C 1s core level, from which we were able to extract the values of three vibrational transitions. These outcomes were in line with the description given by the  $Z + 1$  model. Despite the very small error bar in estimating the position of the different spectral components, the effects of anharmonic nature could not be detected in the vibrational spectra of the core-excited CO. This can be due to three possible causes related to the (i) role of other vibrational modes of the molecule besides the C–O stretching, (ii) contribution of interaction with the supporting substrate, or (iii) surface inhomogeneity effects.

## ASSOCIATED CONTENT

### Supporting Information

The Supporting Information is available free of charge at <https://pubs.acs.org/doi/10.1021/acs.jpcc.1c09646>.

Dependence of C 1s on the photon energy, LEED patterns acquired on the two different CO adsorbate layers, and C 1s evolution during CO uptake (PDF)

## AUTHOR INFORMATION

### Corresponding Author

Alessandro Baraldi – Department of Physics, University of Trieste, 34127 Trieste, Italy; Elettra Sincrotrone Trieste, 34149 Trieste, Italy; [orcid.org/0000-0001-5690-9668](https://orcid.org/0000-0001-5690-9668); Email: [baraldi@elettra.eu](mailto:baraldi@elettra.eu)

## Authors

Stefania Baronio – Department of Physics, University of Trieste, 34127 Trieste, Italy  
Valeria De Leo – Department of Physics, University of Trieste, 34127 Trieste, Italy  
Ginevra Lautizi – Department of Physics, University of Trieste, 34127 Trieste, Italy  
Paola Mantegazza – Department of Physics, University of Trieste, 34127 Trieste, Italy  
Eleonora Natale – Department of Physics, University of Trieste, 34127 Trieste, Italy  
Manuel Tuniz – Department of Physics, University of Trieste, 34127 Trieste, Italy  
Stefano Vigneri – Department of Physics, University of Trieste, 34127 Trieste, Italy  
Luca Bignardi – Department of Physics, University of Trieste, 34127 Trieste, Italy; [orcid.org/0000-0002-9846-9100](https://orcid.org/0000-0002-9846-9100)  
Paolo Lacovig – Elettra Sincrotrone Trieste, 34149 Trieste, Italy; [orcid.org/0000-0001-7001-7930](https://orcid.org/0000-0001-7001-7930)  
Silvano Lizzit – Elettra Sincrotrone Trieste, 34149 Trieste, Italy; [orcid.org/0000-0003-1620-7228](https://orcid.org/0000-0003-1620-7228)

Complete contact information is available at: <https://pubs.acs.org/10.1021/acs.jpcc.1c09646>

## Notes

The authors declare no competing financial interest.

## ACKNOWLEDGMENTS

The authors thank Elettra-Sincrotrone Trieste for providing access to the Elettra laboratory and for the support received during the beamtime allocated at the SuperESCA beamline. Financial support from the Department of Physics of the University of Trieste is gratefully acknowledged.

## REFERENCES

- (1) Gelius, U.; Basilier, E.; Svensson, S.; Bergmark, T.; Siegbahn, K. A high resolution ESCA instrument with X-ray monochromator for gases and solids. *J. Electron Spectrosc. Relat. Phenom.* **1973**, *2*, 405–434.
- (2) Gelius, U. Recent progress in ESCA studies of gases. *J. Electron Spectrosc. Relat. Phenom.* **1974**, *5*, 985–1057.
- (3) Gelius, U.; Svensson, S.; Siegbahn, H.; Basilier, E.; Faxälv, Å.; Siegbahn, K. Vibrational and lifetime line broadenings in ESCA. *Chem. Phys. Lett.* **1974**, *28*, 1–7.
- (4) Randall, K. J.; Kilcoyne, A. L. D.; Köppe, H. M.; Feldhaus, J.; Bradshaw, A. M.; Rubensson, J. E.; Eberhardt, W.; Xu, Z.; Johnson, P. D.; Ma, Y. Photon energy dependence of the high resolution C 1s photoelectron spectrum of CO in the threshold region. *Phys. Rev. Lett.* **1993**, *71*, 1156–1159.
- (5) Medhurst, L.; Heimann, P.; Siggel, M.; Shirley, D.; Chen, C.; Ma, Y.; Modesti, S.; Sette, F. Vibrationally resolved threshold photoemission of N<sub>2</sub> and CO at the N and C K-edges. *Chem. Phys. Lett.* **1992**, *193*, 493–498.
- (6) Andersen, J.; Beutler, A.; Sorensen, S.; Nyholm, R.; Setlik, B.; Heskett, D. Vibrational fine structure in the C 1s core level photoemission of chemisorbed molecules: ethylene and ethylidyne on Rh(111). *Chem. Phys. Lett.* **1997**, *269*, 371–377.
- (7) Fuhrmann, T.; Kinne, M.; Whelan, C.; Zhu, J.; Denecke, R.; Steinrück, H.-P. Vibrationally resolved in situ XPS study of activated adsorption of methane on Pt(111). *Chem. Phys. Lett.* **2004**, *390*, 208–213.
- (8) Fuhrmann, T.; Kinne, M.; Tränkenschuh, B.; Papp, C.; Zhu, J. F.; Denecke, R.; Steinrück, H.-P. Activated adsorption of methane on Pt(111) - an in situ XPS study. *New J. Phys.* **2005**, *7*, 107.

- (9) Larciprete, R.; Goldoni, A.; Grošo, A.; Lizzit, S.; Paolucci, G. The photochemistry of CH<sub>4</sub> adsorbed on Pt(111) studied by high resolution fast XPS. *Surf. Sci.* **2001**, *482–485*, 134–140.
- (10) Neubauer, R.; Whelan, C. M.; Denecke, R.; Steinrück, H.-P. The thermal chemistry of saturated layers of acetylene and ethylene on Ni(100) studied by in situ synchrotron x-ray photoelectron spectroscopy. *J. Chem. Phys.* **2003**, *119*, 1710–1718.
- (11) Steinrück, H.-P.; Fuhrmann, T.; Papp, C.; Tränkenschuh, B.; Denecke, R. A detailed analysis of vibrational excitations in x-ray photoelectron spectra of adsorbed small hydrocarbons. *J. Chem. Phys.* **2006**, *125*, 204706.
- (12) Wiklund, M.; Jaworowski, A.; Strisland, F.; Beutler, A.; Sandell, A.; Nyholm, R.; Sorensen, S.; Andersen, J. Vibrational fine structure in the C1s photoemission spectrum of the methoxy species chemisorbed on Cu(100). *Surf. Sci.* **1998**, *418*, 210–218.
- (13) Wiklund, M.; Beutler, A.; Nyholm, R.; Andersen, J. Vibrational analysis of the C 1s photoemission spectra from pure ethylidyne and ethylidyne coadsorbed with carbon monoxide on Rh(111). *Surf. Sci.* **2000**, *461*, 107–117.
- (14) Föhlisch, A.; Wassdahl, N.; Hasselström, J.; Karis, O.; Menzel, D.; Mårtensson, N.; Nilsson, A. Beyond the Chemical Shift: Vibrationally Resolved Core-Level Photoelectron Spectra of Adsorbed CO. *Phys. Rev. Lett.* **1998**, *81*, 1730–1733.
- (15) Föhlisch, A.; Hasselström, J.; Karis, O.; Väterlein, P.; Mårtensson, N.; Nilsson, A.; Heske, C.; Stichler, M.; Keller, C.; Wurth, W.; et al. Franck–Condon breakdown in core-level photoelectron spectroscopy of chemisorbed CO. *Chem. Phys. Lett.* **1999**, *315*, 194–200.
- (16) Smedh, M.; Beutler, A.; Ramsvik, T.; Nyholm, R.; Borg, M.; Andersen, J.; Duschek, R.; Sock, M.; Netzer, F.; Ramsey, M. Vibrationally resolved C 1s photoemission from CO adsorbed on Rh(111): the investigation of a new chemically shifted C 1s component. *Surf. Sci.* **2001**, *491*, 99–114.
- (17) Ramsvik, T.; Borg, A.; Kildemo, M.; Raaen, S.; Matsuura, A.; Jaworowski, A.; Worren, T.; Leandersson, M. Molecular vibrations in core-ionised CO adsorbed on Co(0001) and Rh(100). *Surf. Sci.* **2001**, *492*, 152–160.
- (18) Surnev, S.; Sock, M.; Ramsey, M.; Netzer, F.; Wiklund, M.; Borg, M.; Andersen, J. CO adsorption on Pd(111): a high-resolution core level photoemission and electron energy loss spectroscopy study. *Surf. Sci.* **2000**, *470*, 171–185.
- (19) von Schenck, H.; Janin, E.; Tjernberg, O.; Svensson, M.; Göthelid, M. CO bonding on tin modified Pt(110)-(1 × 2). *Surf. Sci.* **2003**, *526*, 184–192.
- (20) Baraldi, A.; Comelli, G.; Lizzit, S.; Kiskinova, M.; Paolucci, G. Real-time X-ray photoelectron spectroscopy of surface reactions. *Surf. Sci. Rep.* **2003**, *49*, 169–224.
- (21) Huber, K. P.; Herzberg, G. *Molecular Spectra and Molecular Structure, IV. Constants of Diatomic Molecules* **1979**, DOI: 10.1007/978-1-4757-0961-2.
- (22) Rank, D. H.; Guenther, A. H.; Saksena, G. D.; Shearer, J. N.; Wiggins, T. A. Tertiary Interferometric Wavelength Standards from Measurements on Lines of the 2–0 Band of Carbon Monoxide and Derived Wavelength Standards for Some Lines of the 1–0 Band of Carbon Monoxide The Velocity of Light Derived from a Band Spectrum Method IV\*. *J. Opt. Soc. Am.* **1957**, *47*, 686.
- (23) Comrie, C. M.; Weinberg, W. H. The chemisorption of carbon monoxide on the iridium (III) surface. *J. Chem. Phys.* **1976**, *64*, 250–259.
- (24) Bianchi, M.; Cassese, D.; Cavallin, A.; Comin, R.; Orlando, F.; Postregna, L.; Golfetto, E.; Lizzit, S.; Baraldi, A. Surface core level shifts of clean and oxygen covered Ir(111). *New J. Phys.* **2009**, *11*, 063002.
- (25) Lacovig, P.; Pozzo, M.; Alfè, D.; Vilmercati, P.; Baraldi, A.; Lizzit, S. Growth of Dome-Shaped Carbon Nanoislands on Ir(111): The Intermediate between Carbide Clusters and Quasi-Free-Standing Graphene. *Phys. Rev. Lett.* **2009**, *103*, 166101.
- (26) Doniach, S.; Sunjic, M. Many-electron singularity in X-ray photoemission and X-ray line spectra from metals. *J. Phys. C: Solid State Phys.* **1970**, *3*, 285–291.
- (27) Boyle, R. W.; Lauterbach, J.; Schick, M.; Mitchell, W. J.; Weinberg, W. H. Chemisorption of Carbon Monoxide on the Iridium(111) Surface: In Situ Studies of Adsorption and Desorption Kinetics via Vibrational Spectroscopy. *Ind. Eng. Chem. Res.* **1996**, *35*, 2986–2992.
- (28) Lauterbach, J.; Boyle, R.; Schick, M.; Mitchell, W.; Meng, B.; Weinberg, W. The adsorption of CO on Ir(111) investigated with FT-IRAS. *Surf. Sci.* **1996**, *350*, 32–44.
- (29) Li, X.; Pramhaas, V.; Rameshan, C.; Blaha, P.; Rupprechter, G. Coverage-Induced Orientation Change: CO on Ir(111) Monitored by Polarization-Dependent Sum Frequency Generation Spectroscopy and Density Functional Theory. *J. Phys. Chem. C* **2020**, *124*, 18102–18111.
- (30) Liu, C.; Zhu, L.; Ren, P.; Wen, X.; Li, Y.-W.; Jiao, H. High-Coverage CO Adsorption and Dissociation on Ir(111), Ir(100), and Ir(110) from Computations. *J. Phys. Chem. C* **2019**, *123*, 6487–6495.
- (31) Tadele, K.; Zhang, Q.; Mohammed, L. Molecular and dissociative adsorption of CO and SO on the surface of Ir(111). *AIP Adv.* **2020**, *10*, 035021.
- (32) Gajdoš, M.; Eichler, A.; Hafner, J. CO adsorption on close-packed transition and noble metal surfaces: trends from ab initio calculations. *J. Phys.: Condens. Matter* **2004**, *16*, 1141.
- (33) German, E. D.; Sheintuch, M. Comparative Theoretical Study of CO Adsorption and Desorption Kinetics on (111) Surfaces of Transition Metals. *J. Phys. Chem. C* **2008**, *112*, 14377–14384.
- (34) Krekelberg, W. P.; Greeley, J.; Mavrikakis, M. Atomic and Molecular Adsorption on Ir(111). *J. Phys. Chem. B* **2004**, *108*, 987–994.
- (35) Liu, C.; Zhu, L.; Ren, P.; Wen, X.; Li, Y.-W.; Jiao, H. High-Coverage CO Adsorption and Dissociation on Ir(111), Ir(100), and Ir(110) from Computations. *J. Phys. Chem. C* **2019**, *123*, 6487–6495.
- (36) Bondino, F.; Comelli, G.; Esch, F.; Locatelli, A.; Baraldi, A.; Lizzit, S.; Paolucci, G.; Rosei, R. Structural determination of molecules adsorbed in different sites by means of chemical shift photoelectron diffraction: c(4 × 2)-CO on Pt(111). *Surf. Sci.* **2000**, *459*, L467–L474.
- (37) McEwen, J.-S.; Payne, S.; Kreuzer, H. J.; Kinne, M.; Denecke, R.; Steinrück, H.-P. Adsorption and desorption of CO on Pt(111): a comprehensive analysis. *Surf. Sci.* **2003**, *545*, 47–69.
- (38) Kinne, M.; Fuhrmann, T.; Whelan, C.; Zhu, J.; Pantförder, J.; Probst, M.; Held, G.; Denecke, R.; Steinrück, H.-P. Kinetic parameters of CO adsorbed on Pt (111) studied by in situ high resolution x-ray photoelectron spectroscopy. *J. Chem. Phys.* **2002**, *117*, 10852–10859.
- (39) Baraldi, A.; Lizzit, S.; Comelli, G.; Kiskinova, M.; Rosei, R.; Honkala, K.; Nørskov, J. K. Spectroscopic Link between Adsorption Site Occupation and Local Surface Chemical Reactivity. *Phys. Rev. Lett.* **2004**, *93*, 046101.
- (40) Osterwalder, J. In *Surface and Interface Science*; Wandelt, K., Ed.; John Wiley & Sons, Ltd.: 2013; Chapter 3.2, pp 151–214.
- (41) Baraldi, A. Structure and chemical reactivity of transition metal surfaces as probed by synchrotron radiation core level photoelectron spectroscopy. *J. Phys.: Condens. Matter* **2008**, *20*, 093001.
- (42) Björneholm, O.; Nilsson, A.; Tillborg, H.; Bennich, P.; Sandell, A.; Hernnäs, B.; Puglia, C.; Mårtensson, N. Overlayer structure from adsorbate and substrate core level binding energy shifts: CO, CCH<sub>3</sub> and O on Pt(111). *Surf. Sci.* **1994**, *315*, L983–L989.
- (43) Santucci, S. C.; Goldoni, A.; Larciprete, R.; Lizzit, S.; Bertolo, M.; Baraldi, A.; Masciovecchio, C. Calorimetry at Surfaces Using High-Resolution Core-Level Photoemission. *Phys. Rev. Lett.* **2004**, *93*, 106105.
- (44) Baraldi, A.; Comelli, G.; Lizzit, S.; Rosei, R.; Paolucci, G. Effects of the interatomic-potential anharmonicity on the bulk and surface photoemission core levels. *Phys. Rev. B* **2000**, *61*, 12713–12716.



(45) Bianchettin, L.; Baraldi, A.; de Gironcoli, S.; Vesselli, E.; Lizzit, S.; Petaccia, L.; Comelli, G.; Rosei, R. Core level shifts of undercoordinated Pt atoms. *J. Chem. Phys.* **2008**, *128*, 114706.

(46) Miniussi, E.; Hernández, E. R.; Pozzo, M.; Baraldi, A.; Vesselli, E.; Comelli, G.; Lizzit, S.; Alfé, D. Non-local Effects on Oxygen-Induced Surface Core Level Shifts of Re(0001). *J. Phys. Chem. C* **2012**, *116*, 23297–23307.

(47) Ferrari, E.; Galli, L.; Miniussi, E.; Morri, M.; Panighel, M.; Ricci, M.; Lacovig, P.; Lizzit, S.; Baraldi, A. Layer-dependent Debye temperature and thermal expansion of Ru(0001) by means of high-energy resolution core-level photoelectron spectroscopy. *Phys. Rev. B* **2010**, *82*, 195420.

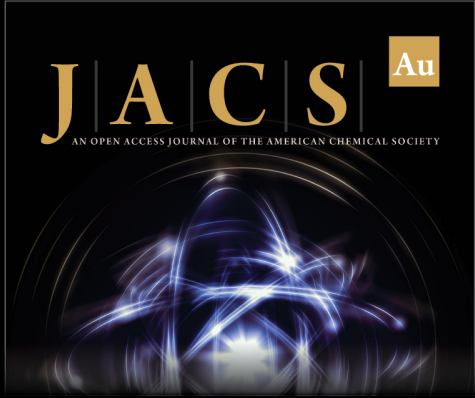
(48) Cornish, J. C.; Avery, N. R. Adsorption of N<sub>2</sub>, O<sub>2</sub>, N<sub>2</sub>O and NO on Ir (111) by EELS and TPD. *Surf. Sci.* **1990**, *235*, 209–216.

(49) Fujitani, T.; Nakamura, I.; Kobayashi, Y.; Takahashi, A.; Haneda, M.; Hamada, H. Adsorption and reactions of NO on clean and CO-precovered Ir (111). *J. Phys. Chem. B* **2005**, *109*, 17603–17607.


(50) Carroll, T. X.; Børve, K. J.; Sæthre, L. J.; Bozek, J. D.; Kukk, E.; Hahne, J. A.; Thomas, T. D. Carbon 1s photoelectron spectroscopy of CF<sub>4</sub> and CO: Search for chemical effects on the carbon 1s hole-state lifetime. *J. Chem. Phys.* **2002**, *116*, 10221–10228.


(51) Hergenhahn, U. Vibrational structure in inner shell photoionization of molecules. *J. Phys. B: At. Mol. Opt. Phys.* **2004**, *37*, R89.


(52) Osborne, S. J.; Sundin, S.; Ausmees, A.; Svensson, S.; Saethre, L. J.; Svaeren, O.; Sorensen, S. L.; Végh, J.; Karvonen, J.; Aksela, S.; et al. The vibrationally resolved C 1s core photoelectron spectra of methane and ethane. *J. Chem. Phys.* **1997**, *106*, 1661–1668.



**JACS** Au  
AN OPEN ACCESS JOURNAL OF THE AMERICAN CHEMICAL SOCIETY

 Editor-in-Chief  
**Prof. Christopher W. Jones**  
Georgia Institute of Technology, USA

**Open for Submissions** 

pubs.acs.org/jacsau  ACS Publications  
Most Trusted. Most Cited. Most Read.